Geophys. J. Int. (2002) **150,** 800–808

Seismogram synthesis for piecewise heterogeneous media

Li-Yun Fu*

Institute of Tectonics, University of California at Santa Cruz, 1156 High Stree, Santa Cruz, CA 95064, *USA. E-mail: li-yun.fu@csiro.au*

Accepted 2002 April 4. Received 2002 March 1; in original form 2001 October 11

SUMMARY

We present a semi-analytical, semi-numerical method to simulate wave propagation in piecewise heterogeneous media that the Earth presents. Wave propagation in such media will highlight the reflections/transmissions at interfaces, while the volume heterogeneities in each geological formation generate scattered waves that are superimposed on the boundary waves to cause fluctuations in amplitude and phase. The numerical method is a straightforward extension to irregular multilayered media of the generalized Lipmann-Schwinger integral equation formulated in terms of volume scattering and boundary scattering. Compared to the finite-difference and finite-element methods for heterogeneous media, the boundary-volume integral equation technique enjoys a distinct characteristic of the explicit use of the boundary conditions of continuities for displacement and traction across subsurface interfaces, which provides sufficient accuracy for simulating the reflection/transmission across irregular interfaces. The resultant global coefficient matrix is sparse and narrow-banded. We discuss several aspects of seismic modeling implementation in order to make the calculations more efficient. The accuracy of the method is tested by comparing with the analytical solutions for a semicircular alluvial valley, which confirms that sampling at three elements per wavelength is sufficient to ensure the accuracy for general applications. To show the applicability of the method, we calculated synthetic seismograms that show significant impact of volume heterogeneities on seismic responses in a layered medium system.

Key words: boundary-volume integral equation technique, generalized Lipmann-Schwinger integral equation, piecewise heterogeneous media, wave propagation.

INTRODUCTION

Most geological formations are strongly stratified with fairly smooth lateral variations in medium property within each formation. In this layered media, the mean properties of the media are strong contrast between layers, while volume heterogeneities inside each layer can be described as deviations from the mean values. Wave propagation through such piecewise heterogeneous media will dominate the reflection/transmission across subsurface interfaces, while the scattered waves by volume heterogeneities are superimposed on the boundary waves and lead to, at seismic frequencies, moderate fluctuations in amplitude and phase of the resultant field. This implies that wave propagation simulation through such media may prefer some exclusive methods that somewhat differ from general numerical modeling techniques. The key issues for such candidate methods are (1) the geometrically accurate description of irregular interfaces, (2) the explicit use of the boundary conditions of continuities for displacement and traction across interfaces, (3) the ability to deal with spatial fluctuations and subtle scattering effects of volume heterogeneities inside each formation.

Indeed, the finite-difference (FD) and finite-element (FE) methods are often thought of as general tools for the complete solution to problems of wave propagation in arbitrarily varying media. However, these methods do not explicitly consider the boundary continuity conditions between different formations. That disables the methods to sufficient accuracy for modeling the reflection/transmission across irregular interfaces. Numerical errors involved may produce effects so large that are comparable to those caused by attenuation, dispersion, and anisotropy predicted by scattering theory (Wu 1989). Therefore, numerical modeling schemes have to be highly accurate to yield reliable results about both subtle reflection/transmission effects across interfaces and subtle scattering effects from volume heterogeneities inside each formation. In contrast to the regular gridding in the FD method, the FE method allows spatial sampling to vary with the local complexity of the media. This flexibility makes the method more reliable to model irregular interfaces. However, both the FD and FE methods are characteristic

*Now at: CSIRO Petroleum, Suite 5, Petroleum House, 3 Brodie Hall Drive, Technology Park, Bentley WA 6102, Australia.

of the implicit use of boundary conditions, while the explicit use will lead to a category of semi-analytical and semi-numerical methods that may be more important for the reflection/transmission simulation across irregular interfaces. The purpose of this paper is to develop an accurate and efficient seismic modeling method for wave propagation in piecewise heterogeneous media. We demonstrate its suitability to comply with the three special requirements mentioned above.

Targeted at wave propagation in layered media, numerical modeling techniques with an explicit use of boundary continuity conditions have been extensively studied. The boundary integral equation-discrete wavenumber method (Bouchon *et al.* 1989) provides a full-wave solution for multilayered media having irregular interfaces. This method incorporates the discrete wavenumber Green's function representation into the boundary integral equation techniques so that the evaluation of the singular integrals associated with the Green's function can be avoided. Kennett (1984) presented a coupled mode method where the propagator can be broken down into contributions associated with particular wavetypes. It can be modified to incorporate moderately heterogeneous media. Chen (1990) combined the wavefield plane-wave expansion, the discrete wavenumber Green's function representation, and the boundary integral equation to develop a global generalized reflection/transmission matrices method for irregular layered media. This method can be viewed as an extension of the generalized R/T coefficients method (Kennett 1983) developed for horizontally layered media to irregular layered ones. However, the presence of general volume heterogeneities inside each layer precludes the applicability of these plane-wave decomposition methods. In general, the volume heterogeneities lead to a coupled boundary-volume interaction that requires an extension of traditional boundary methods to account for volume heterogeneities.

Fu *et al.* (1997) developed a numerical method to solve the Lipmann-Schwinger integral equation for numerical wave propagation in volume heterogeneous media. By incorporating the boundary integral representation into the Lipmann-Schwinger integral equation, the method was then extended (Fu 2001) to study the influence of widely observed strong scattered noises caused by rugged topographies and strong volume heterogeneities in complex near-surface areas. In the present work we extend the generalized Lipmann-Schwinger integral equation numerical method to heterogeneous layered media having irregular interfaces. The method provides an efficient scheme to synthesize seismograms in piecewise heterogeneous media by the explicit use of boundary continuity conditions across subsurface interfaces. The scattering term associated with volume integrals over volume heterogeneities can be calculated by accurate Gaussian integration numerical algorithms, which guarantees an optimum seismic modeling for scattering effects by volume heterogeneities with arbitrary complexity. The presentation is restricted to antiplane motion (*SH* waves), which is similar to the acoustic case. The generalization of the scheme to the elastic case is straightforward. Although this boundary-volume integral equation numerical technique can be a powerful tool for piecewise heterogeneous media, the computation becomes extremely time intensive due to the very large size of the resulting matrices to be inverted when the ratio of model dimension to wavelength becomes too large. Consequently the technique is limited to small problems or low frequencies. Several aspects are considered in the paper to make the algorithm implementation more efficient. However, the resulting improvement in computing speed is not significant for large problems. Much faster solutions might be obtained by incorporating a fast multipole method that has been used to solve boundary integral equations for 3-D electromagnetic scattering problems (Coifman *et al.* 1993) and for 3-D elastic wave scattering problems (Fujiwara 2000). Applying the fast multipole method to the boundary-volume integral equation for piecewise heterogeneous media will be conducted in the future.

SIMULTANEOUS INTEGRAL EQUATIONS FOR MULTILAYERED MEDIA

Problem definition

Wave propagation in a large-scale boundary structure with internal volume heterogeneities can be described by a generalized Lipmann-Schwinger integral equation (GLSIE). It is formulated as the superposition of incident, boundary-scattering, and volume-scattering waves. In this section we extend the GLSIE representation to multilayered media with each layer being different scale heterogeneities. The problem to be studied is illustrated in Fig. 1. In this model, there are N heterogeneous layers $V^{(i)}(i = 1, 2, \ldots, N)$ over a half-space, among which the ith layer is bounded by two irregular interfaces $\partial V^{(i-1)}$ and $\partial V^{(i)}$. The uppermost interface is a free surface, and an arbitrary source is embedded in the sth layer. For simplicity, we restrict the present study to the 2-D *SH* problem (or acoustic problem). The elastic properties of each layer are described by the shear modulus $\mu^{(i)}(\mathbf{r})$ and density $\rho^{(i)}(\mathbf{r})$ with the corresponding reference values $\mu_0^{(i)}$ and $\rho_0^{(i)}$. The solution domain of the problem for the ith layer is defined as $\bar{V}^{(i)} \in V^{(i)} + \partial V^{(i-1)} + \partial V^{(i)}$. Seismic response $u(\mathbf{r})$ for steady state scalar wave propagation in the ith layer satisfies the following scalar equation

$$\nabla^2 u(\mathbf{r}) + \left(k^{(i)}(\mathbf{r})\right)^2 u(\mathbf{r}) = -\delta_{si} s(\mathbf{r}, \omega), \mathbf{r} \in \bar{V}^{(i)} \quad i = 1, 2, \ldots, N, \tag{1}$$

where the wavenumber $(k^{(i)}(\mathbf{r}))^2 = \omega^2 \rho^{(i)}(\mathbf{r})/\mu^{(i)}(\mathbf{r})$with the corresponding reference wavenumber $(k_0^{(i)})^2 = \omega^2 \rho_0^{(i)}/\mu_0^{(i)}$, $\delta_{si} = 1$ for $i = s$ and $\delta_{si} = 0$ for $i \neq s$, and $s(\mathbf{r}, \omega)$ is the body force. The seismic response $u(\mathbf{r})$ also satisfies the following boundary conditions: 1) the traction-free condition on the free surface: $\partial u(\mathbf{r})/\partial n = 0$ at $\mathbf{r} \in \partial V^{(0)}$, 2) the continuities of displacement and traction at the interboundary between $V^{(i)}$ and $V^{(i+1)}$

$$\begin{cases} u^{(i)}(\mathbf{r}) = u^{(i+1)}(\mathbf{r}) \\ \mu^{(i)} \dfrac{\partial u^{(i)}(\mathbf{r})}{\partial n} = \mu^{(i+1)} \dfrac{\partial u^{(i+1)}(\mathbf{r})}{\partial n}, \quad \mathbf{r} \in \partial V^{(i)} \end{cases}, \tag{2}$$

and 3) the radiation boundary conditions imposed on the far-field behaviour at infinity

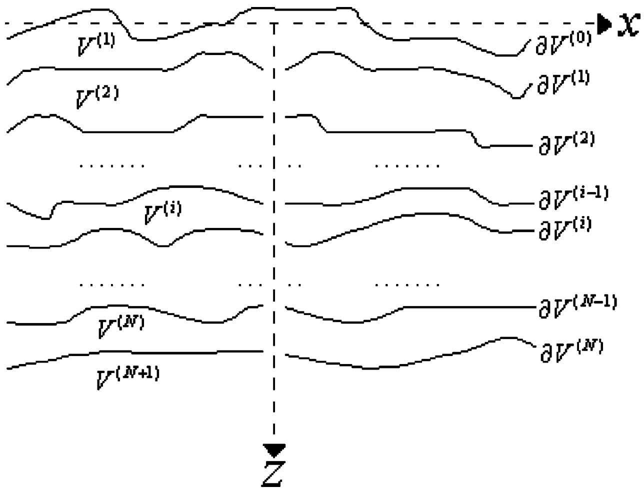

Figure 1. Configuration of the problem considered.

$$\begin{cases} \lim\limits_{|r|\to\infty} u(\mathbf{r}) = 0 \\ \lim\limits_{|r|\to\infty} \dfrac{\partial u(\mathbf{r})}{\partial r} = 0 \end{cases}. \tag{3}$$

Boundary-volume integral equation representation

To explicitly use the boundary conditions defined by eq. (2) in the solution of the problem, we need to transform eq. (1) into an integral equation in terms of boundary and volume integrals of the solution domain. Supposing the source point is located at $\mathbf{r}_0$, the source term can be expressed as $s(\mathbf{r}, \omega) = S(\omega)\delta(\mathbf{r} - \mathbf{r}_0)$, where $S(\omega)$ is the source spectrum and $\delta(\mathbf{r} - \mathbf{r}_0)$ is the delta function. Defining the relative slowness perturbation $O^{(i)}(\mathbf{r}) = \rho^{(i)}(\mathbf{r})\mu_0^{(i)}/\rho_0^{(i)}\mu^{(i)}(\mathbf{r}) - 1$, we then rewrite eq. (1) with respect to the reference wavenumber

$$\nabla^2 u(\mathbf{r}) + \left(k_0^{(i)}\right)^2 u(\mathbf{r}) = -\delta_{si} S(\omega)\delta(\mathbf{r} - \mathbf{r}_0) - \left(k_0^{(i)}\right)^2 O^{(i)}(\mathbf{r})u(\mathbf{r}). \tag{4}$$

With the aid of the free-space Green's function, eq. (4) can be transformed into the following generalized Lipmann-Schwinger integral equation

$$\begin{aligned} &\int_{\partial V^{(i-1)}} \left[G^{(i)}(\mathbf{r}, \mathbf{r}')t^{(i-1)}(\mathbf{r}') - u^{(i-1)}(\mathbf{r}')\frac{\partial G^{(i)}(\mathbf{r}, \mathbf{r}')}{\partial n} \right] d\mathbf{r}' + \int_{\partial V^{(i)}} \left[G^{(i)}(\mathbf{r}, \mathbf{r}')t^{(i)}(\mathbf{r}') - u^{(i)}(\mathbf{r}')\frac{\partial G^{(i)}(\mathbf{r}, \mathbf{r}')}{\partial n} \right] d\mathbf{r}' \\ &\quad + \left(k_0^{(i)}\right)^2 \int_{V^{(i)}} O^{(i)}(\mathbf{r}')w^{(i)}(\mathbf{r}')G^{(i)}(\mathbf{r}, \mathbf{r}')\, d\mathbf{r}' + \delta_{si} S(\omega)G^{(i)}(\mathbf{r}, \mathbf{r}_0) = \begin{cases} w^{(i)}(\mathbf{r}), & \mathbf{r} \in V^{(i)} \\ C^{(i-1)}(\mathbf{r})u^{(i-1)}(\mathbf{r}), & \mathbf{r} \in \partial V^{(i-1)}, \\ C^{(i)}(\mathbf{r})u^{(i)}(\mathbf{r}), & \mathbf{r} \in \partial V^{(i)} \\ 0, & \text{others} \end{cases} \end{aligned} \tag{5}$$

for all $\mathbf{r}' \in \bar{V}^{(i)}$, where $u^{(i)}(\mathbf{r})$ is the displacement on $\partial V^{(i)}$, $t^{(i)}(\mathbf{r}) = \partial u^{(i)}(\mathbf{r})/\partial n$ the normal gradient of the displacement on $\partial V^{(i)}$, $w^{(i)}(\mathbf{r})$ is the displacement inside $V^{(i)}$, and the coefficients $C(\mathbf{r})$ generally depends on the local geometry at $\mathbf{r}$. The causal Green's function is defined everywhere in the full heterogeneous region $\bar{V}^{(i)}$, relating an 'observation point' $\mathbf{r}$ to a 'scattering point' $\mathbf{r}'$. It satisfies the homogeneous Helmholtz equation in the reference medium

$$\nabla^2 G^{(i)}(\mathbf{r}, \mathbf{r}') + \left(k_0^{(i)}\right)^2 G^{(i)}(\mathbf{r}, \mathbf{r}') = -\delta(\mathbf{r} - \mathbf{r}'), \tag{6}$$

for all $\mathbf{r}, \mathbf{r}' \in \bar{V}^{(i)}$. For 2-D problems, the Green's function is given by

$$G^{(i)}(\mathbf{r}, \mathbf{r}') = \frac{i H_0^{(1)}\left(k_0^{(i)}\left|\mathbf{r}' - \mathbf{r}\right|\right)}{4}, \tag{7}$$

where $i = \sqrt{-1}$ and $H_0^{(1)}$ is the Hankel function of the first kind and of zeroth order. Eq. (5) is a Fredholm integral equation of the second kind. According to the Fredholm's theorems of integral equations, we can prove that the solution of eq. (5) exists and is unique for boundary value problems with both Neumann and Dirichlet boundary conditions. It is worth to mention that formulating wave propagation by integral equations enjoys a unique advantage that eq. (5) naturally satisfies Sommerfeld nonreflecting and decay boundary conditions that are defined by eq. (3) and imposed on the far field behaviour at infinity so that the integrals on artificial boundaries in the model vanish. Therefore, the artificial reflections that arise at the edges of the domain of computation can be avoided by an infinite absorbing element technique (Fu & Wu 2000).

For piecewise homogeneous media (i.e. $O^{(i)}(\mathbf{r}) = 0$), eq. (5) reduces to a standard boundary integral equation that has been further formulated as the boundary integral equation-discrete wavenumber method (Bouchon *et al.* 1989) and global generalized reflection/transmission matrices method (Chen 1990) for multilayered media with irregular interfaces. An efficient alternative is to directly solve the boundary integral equation for multilayered media by the boundary-element (BE) method (Fu 1996). The BE method has been modified to investigate regional wave propagation in Tibet area (Fu & Wu 2001) and for theoretical study of the scattering effects of random topography on regional wave attenuation and amplification (Fu *et al.* 2002). However, these boundary methods are limited by their abilities to handle volume heterogeneities. For piecewise heterogeneous media (i.e. $O^{(i)}(\mathbf{r}) \neq 0$), some flexible approaches have been developed with a great saving of computing time and memory at the cost of accuracy, for example, Schuster (1985) developed a hybrid BEM + Born series modeling scheme to solve multibody scattering problems where perturbed parts with volume integrals can be approximated by a Born series. Wu & Fu (1998)incorporated the BE method and a generalized screen (GS) propagator to model the heterogeneous media where the perturbed parts are solved by the GS method. In this paper we pursue more accurate full-wave solutions for piecewise heterogeneous media. First, the discretization of eq. (5) can be done in each layer by numerical methods such as the collocation method or weighted residual method. Then, all equations are assembled into a set of simultaneous matrix equations by using the boundary conditions of continuity for displacement and traction across all interfaces. This global matrix is sparse or narrow-banded, depending on the structure of the model.

Simultaneous matrix equations

We discretize each interface $\partial V^{(i)}$ into $L^{(i)}$ boundary elements denoted by $\Gamma_e (e = 1, 2, \ldots, L^{(i)})$ and each volume $V^{(i)}$ into $M^{(i)}$ finite elements denoted by $\Omega_e (e = 1, 2, \ldots, M^{(i)})$. The total node number is $NP^{(i)}$. In the collocation method, interpolation shape functions ϕ are used so that the variables ($\mathbf{r}'$, u, t, and w) are approximated by the linear combination of their nodal values over an element Ω_e or Γ_e defined geometrically between the nodes I_1 and I_2, for example,

$$u^{(i)}(\xi) = \sum_{l=I_1}^{I_2} u^{(i)}(\mathbf{r}_l)\phi_l(\xi), \tag{8}$$

where ξ denotes the local coordinate of an element. We then rewrite the integral eq. (5) in operator form

$$H^{(i,1)}u^{(i-1)}(\mathbf{r}_j) - G^{(i,1)}t^{(i-1)}(\mathbf{r}_j) + H^{(i,2)}u^{(i)}(\mathbf{r}_j) - G^{(i,2)}t^{(i)}(\mathbf{r}_j) = K^{(i)}w^{(i)}(\mathbf{r}_j) + \delta_{si} f(\mathbf{r}_j), \quad j = 1, 2, \ldots, NP^{(i)}, \tag{9}$$

where f is the incident field, H and G are the boundary integral operators, and K is the perturbation-domain integral operator. The elements of $H^{(i,1)}$, $G^{(i,1)}$, $H^{(i,2)}$, $G^{(i,2)}$, and $K^{(i)}$ can be computed over elements respectively as

$$h_{jk}^{(i,1)} = \sum_{e=1}^{L^{(i-1)}} \sum_{l=I_1}^{I_2} \left[\int_{\Gamma_e} \frac{\partial}{\partial n} G^{(i)}(\mathbf{r}_j, \mathbf{r}'(\xi))\phi_l(\xi)\, d\mathbf{r}'(\xi) \right] \delta_{lk} + C^{(i-1)}(\mathbf{r}_j)\delta_{jk}, \tag{10}$$

$$g_{jk}^{(i,1)} = \sum_{e=1}^{L^{(i-1)}} \sum_{l=I_1}^{I_2} \left[\int_{\Gamma_e} G^{(i)}(\mathbf{r}_j, \mathbf{r}'(\xi))\phi_l(\xi)\, d\mathbf{r}'(\xi) \right] \delta_{lk}, \tag{11}$$

$$h_{jk}^{(i,2)} = \sum_{e=1}^{L^{(i)}} \sum_{l=I_1}^{I_2} \left[\int_{\Gamma_e} \frac{\partial}{\partial n} G^{(i)}(\mathbf{r}_j, \mathbf{r}'(\xi))\phi_l(\xi)\, d\mathbf{r}'(\xi) \right] \delta_{lk} + C^{(i)}(\mathbf{r}_j)\delta_{jk}, \tag{12}$$

$$g_{jk}^{(i,2)} = \sum_{e=1}^{L^{(i)}} \sum_{l=I_1}^{I_2} \left[\int_{\Gamma_e} G^{(i)}(\mathbf{r}_j, \mathbf{r}'(\xi))\phi_l(\xi)\, d\mathbf{r}'(\xi) \right] \delta_{lk}, \tag{13}$$

and

$$K_{jk}^{(i)} = \sum_{e=1}^{M^{(i)}} \sum_{l=I_1}^{I_2} \left[\left(k_0^{(i)}\right)^2 \int_{\Omega_e} O^{(i)}(\mathbf{r}'(\xi)) G^{(i)}(\mathbf{r}_j, \mathbf{r}'(\xi))\phi_l(\xi)\, d\mathbf{r}'(\xi) \right] \delta_{lk} - \delta_{jk}, \tag{14}$$

where δ_{lk} and δ_{jk} are the Kronecker delta functions, and the Gaussian integration algorithm is used to numerically evaluate these integrals. Eq. (9) can be further compacted as a matrix equation for $j = 1, 2, \ldots, NP^{(i)}$

$$\mathbf{A}^{(i,1)}\mathbf{Q}^{(i-1)} + \mathbf{A}^{(i,2)}\mathbf{Q}^{(i)} = \mathbf{K}^{(i)}\mathbf{v}^{(i)} + \delta_{si}\mathbf{f}, \tag{15}$$

where we define the boundary coefficient matrices $\mathbf{A}^{(i,1)} = [H^{(i,1)}; -G^{(i,1)}]$ and $\mathbf{A}^{(i,2)} = [H^{(i,2)}; -G^{(i,2)}]$, and the unknown boundary displacement-traction vector $\mathbf{Q}^{(i)} = [u^{(i)}; t^{(i)}]$.

We assume that the medium below the layer $V^{(N)}$ is homogeneous, bounded by $\partial V^{(N)}$ and a spherical surface with its radius approach infinity. Letting the source is located in the shallowest layer $V^{(1)}$ as the case in seismic exploration, we can use eq. (15) to build the following global matrix equation that describes wave propagation in the whole model

$$\begin{cases} \mathbf{A}^{(N+1,1)}\mathbf{Q}^{(N)} = 0 \\ \mathbf{A}^{(N,1)}\mathbf{Q}^{(N-1)} + \mathbf{A}^{(N,2)}\mathbf{Q}^{(N)} = \mathbf{K}^{(N)}\mathbf{v}^{(N)} \\ \vdots \\ \mathbf{A}^{(i,1)}\mathbf{Q}^{(i-1)} + \mathbf{A}^{(i,2)}\mathbf{Q}^{(i)} = \mathbf{K}^{(i)}\mathbf{v}^{(i)} \\ \mathbf{A}^{(i-1,1)}\mathbf{Q}^{(i-2)} + \mathbf{A}^{(i-1,2)}\mathbf{Q}^{(i-1)} = \mathbf{K}^{(i-1)}\mathbf{v}^{(i-1)} \\ \vdots \\ \mathbf{A}^{(2,1)}\mathbf{Q}^{(1)} + \mathbf{A}^{(2,2)}\mathbf{Q}^{(2)} = \mathbf{K}^{(2)}\mathbf{v}^{(2)} \\ \mathbf{A}^{(1,1)}\mathbf{Q}^{(0)} + \mathbf{A}^{(1,2)}\mathbf{Q}^{(1)} = \mathbf{K}^{(1)}\mathbf{v}^{(1)} + \mathbf{f} \end{cases}. \tag{16}$$

We see that these matrix equations are coupled in the manner of Markovian chain due to the continuity of the displacement-traction vector across interfaces. Solving the linear equation system (16) results in seismic responses $u(\mathbf{r})$ for all nodes in the medium. The Gaussian elimination algorithms can be used for small-scale problems. For large-scale problems or models with complex geometry, the resultant coefficient matrices are sparse and the simultaneous matrix equations are better to be solved by (1) an improved block Gaussian elimination algorithm if seismic survey is set at the free surface, or (2) conjugate gradient algorithms. Fast algorithm convergence is guaranteed by the system's condition number because the boundary-volume integral formulations often give rise to such coefficient matrices that their magnitudes are always larger for the main diagonal terms.

ALGORITHM CONSIDERATIONS

Algorithm efficiency

Numerical accuracy, computational speed, and memory requirements have been recognized as three key issues to assess a numerical modeling program. The strong dependence of these factors on individual modeling tasks complicates realistic performance analyses. Numerical modelings in geophysics are often made at various frequency scales, for example, ultrasonic frequency, sonic frequency, exploration seismic frequency, and crustal seismic frequency. The media to be modeled are also various at different heterogeneous scales. For practical applications, the trade-off between numerical accuracy and computational efficiency can be made for most modeling tasks. One major drawback of the numerical method presented in this paper is the considerable computer time and memory requirements as indicated clearly by eq. (16). The efficiency of our seismic modeling program depends on (1) the maximum frequency to be calculated, (2) the total number of nodes that depends on elements per wavelength, and (3) the sparsity of the coefficient matrices depending on the geometrical complexity of the used model. In addition, our numerical calculations are performed in the frequency domain, which can be easily vectorized and parallelized. In this section, several aspects are considered in order to make the calculations more efficient.

Improved block Gaussian elimination

For a surface seismic survey we only need to calculate seismic responses at the free surface, which leads to an efficient block Gaussian elimination scheme. Below is a brief description of the scheme for more complicated piecewise heterogeneous media. Fig. 2 shows a complex fault model with different heterogeneous scales in each subregion Ω_i ($i = 1, 2, \ldots, 8$). Applying eq. (15) to each subregion in the order from Ω_8 to Ω_1 leads to a series of matrix equations. The boundary conditions of continuity for displacement and its normal gradient across all interfaces will compact these matrix equations into a global matrix equation system (17) where $\mathbf{A}_{ij}$ is the boundary coefficient submatrix

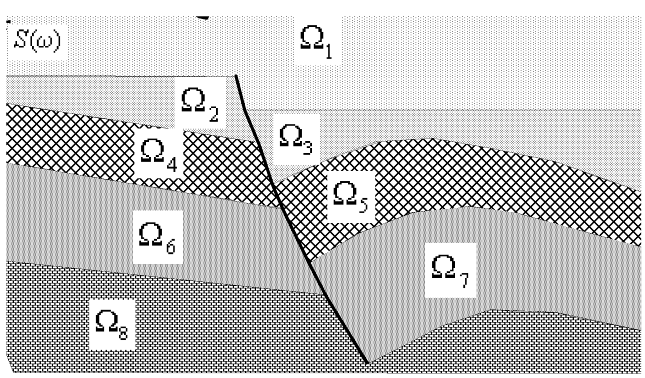

Figure 2. The geometry of a 2-D fault zone model with each subregion being different heterogeneous media. The source $S(\omega)$ is located in the first subregion Ω_1.

obtained by numerical integration over the interboundary between Ω_i and Ω_j, $\mathbf{K}_i$ is the perturbation-domain coefficient submatrix of Ω_i, and $\mathbf{m}_i = [\mathbf{w}^{(i)}; \mathbf{u}^{(i)}; \mathbf{t}^{(i)}]$ is the solution vector at all nodes of Ω_i. There are three characteristics presenting in eq. (17), which will facilitate the solution of this equation system by the great saving of computing time and memory. First, the global coefficient matrix is narrow, sparse, and block-banded. Secondly, the source term $\mathbf{f}$ occurs in the last row because the source point is located at $\mathbf{r}_0 \in \Omega_1$. For multisource modeling, $\mathbf{m}_i$ and $\mathbf{f}$ become matrices but $\mathbf{A}_{ij}$ keeps unchanged. Thirdly, solving the eq. (11) is only for $\mathbf{m}_1$ if seismic observation is limited in the near-surface region Ω_1. That is, we do not need to keep the coefficient matrices for $\mathbf{m}_2, \mathbf{m}_3, \ldots, \mathbf{m}_8$ in memory after each time of Gaussian elimination.

Based on these characteristics, an improved block Gaussian elimination scheme is developed to solve eq. (17) for $\mathbf{m}_1$. The numerical integration, assembly, and elimination of the coefficient matrices are performed subregion by subregion orderly from Ω_8 to Ω_1. Each time of elimination can eliminate the coupling data of the interboundary between two adjoining subregions. This process continues until the surface subregion Ω_1 is reached, resulting in a final coefficient matrix with its dimension determined only by the nodal number in Ω_1. This matrix implicitly contains information of wave propagation through the whole model. Associating this matrix with surface multiline and multisource survey, one will be able to calculate observed fields anywhere inside Ω_1. During the whole computational procedure, the maximum memory required for the global coefficient matrix is always limited to the total nodal number in the largest subregion.

$$\begin{bmatrix}
\mathbf{K}_8 & \mathbf{A}_{87} & \mathbf{A}_{86} & & & & & & & & & & & & & & & & & & & \\
 & \mathbf{A}_{78} & \mathbf{0} & \mathbf{K}_7 & \mathbf{A}_{76} & \mathbf{A}_{75} & & & & & & & & & & & & & & & & \\
 & & \mathbf{A}_{68} & \mathbf{0} & \mathbf{A}_{67} & \mathbf{0} & \mathbf{K}_6 & \mathbf{A}_{65} & \mathbf{A}_{64} & & & & & & & & & & & & & \\
 & & & & & \mathbf{A}_{57} & \mathbf{0} & \mathbf{A}_{56} & \mathbf{0} & \mathbf{K}_5 & \mathbf{A}_{54} & \mathbf{A}_{53} & & & & & & & & & & \\
 & & & & & & & & \mathbf{A}_{46} & \mathbf{0} & \mathbf{A}_{45} & \mathbf{0} & \mathbf{K}_4 & \mathbf{A}_{43} & \mathbf{A}_{42} & & & & & & & \\
 & & & & & & & & & & & \mathbf{A}_{35} & \mathbf{0} & \mathbf{A}_{34} & \mathbf{0} & \mathbf{K}_3 & \mathbf{A}_{32} & \mathbf{A}_{31} & & & & \\
 & & & & & & & & & & & & & & \mathbf{A}_{24} & \mathbf{0} & \mathbf{A}_{23} & \mathbf{0} & \mathbf{K}_2 & \mathbf{A}_{21} & & \\
 & & & & & & & & & & & & & & & & & \mathbf{A}_{13} & \mathbf{0} & \mathbf{A}_{12} & \mathbf{K}_1 & \mathbf{A}_{10}
\end{bmatrix}
\begin{bmatrix} \mathbf{m}_8 \\ \mathbf{m}_7 \\ \mathbf{m}_6 \\ \mathbf{m}_5 \\ \mathbf{m}_4 \\ \mathbf{m}_3 \\ \mathbf{m}_2 \\ \mathbf{m}_1 \end{bmatrix}
=
\begin{bmatrix} \mathbf{0} \\ \mathbf{0} \\ \mathbf{0} \\ \mathbf{0} \\ \mathbf{0} \\ \mathbf{0} \\ \mathbf{0} \\ \mathbf{f} \end{bmatrix} \tag{17}$$

Elements per wavelength

Fewer elements per wavelength will reduce the size of the resultant coefficient matrices. For the boundary integral-discrete wavenumber method, Campillo (1987) found that a discretization rate of three points per wavelength is sufficient to make the numerical noise level negligible. Furthermore, Bouchon *et al.* (1989) compared the method with the plane-wave reflection and transmission coefficient method for a flat-layered medium and verified the method's accuracy at a sampling rate of three points wavelength. To test the accuracy of our seismic modeling program and also determine an applicable element number per wavelength, we compare our numerical solution with the exact solution of scattering for a semicircular alluvial valley of radius a (see Fig. 3). The excitation is in the half-space with an infinite train of incident harmonic plane waves controlled by frequency ω and the angle of incidence θ measured from the vertical axis. Seismic responses are recorded on the free surface. Because of geometric simplicity, the problem can be solved exactly in closed form. The analytical solution in the frequency domain has been studied by Trifunac (1971) for understanding of the role of surface topography. Although the model is one of the simplest, the two sharp edges at $x = \pm a$ in the model provide a crucial target to test various numerical methods. Fig. 4 presents a comparison between the analytical solutions (Trifunac 1971) and our results calculated using various sampling rates for the dimensionless frequencies $\eta = 1$. The dimensionless frequency is defined as $\eta = 2a/\lambda$, where λ is the wavelength of incident waves. The remarkable agreement between the two solutions shows the validity of our computation program and also confirms that sampling at three elements per wavelength is sufficient to ensure the accuracy of the results, even though the elements are too few to represent the shape of the arc of the semicircular alluvial valley. Using two elements per wavelength will reduce accuracy for two receivers at $x = \pm a$. Because the wavelength is the function of frequencies, a variable element dimension technique can be adopted in the program implementation (Fu 1996) to improve

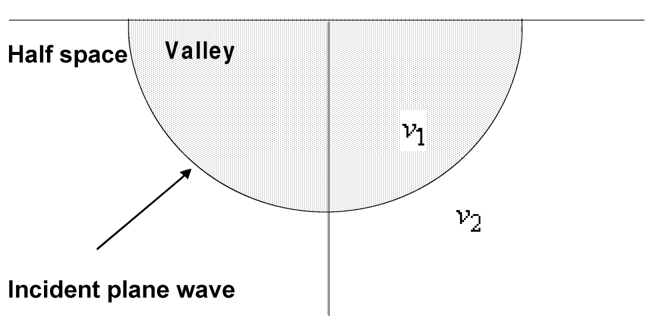

Figure 3. Geometry of a semicircular valley with the radius a and the velocity v_1 in the half space of velocity v_2. The excitation is in the half-space with an infinite train of incident harmonic plane waves of frequency ω and angle θ.

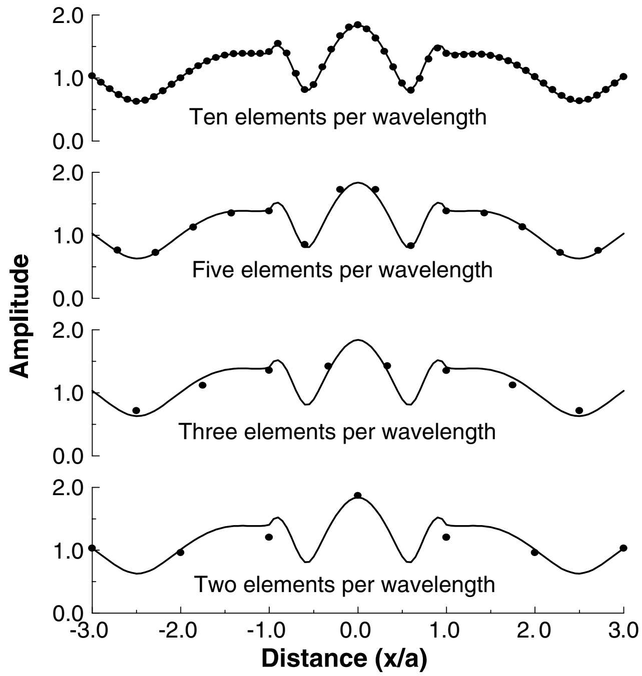

Figure 4. The frequency responses of the semicircular valley (see Fig. 3) to 0^0 incident harmonic plane wave with the dimensionless frequencies $\eta = 1$. The solid lines denote the exact solutions (Trifunac 1971) and the dots denote our results for various sampling rates. It confirms that sampling at three elements per wavelength is sufficient to ensure the accuracy of the results.

computation speed. The element dimension for each frequency is computed according to the medium velocity and the frequency, and then the model is automatically discretized.

Bouchon's sparsity approximation

The boundary-volume integral formulation for a large-scale model with complex geometry will produce a sparse matrix equation system. For some problems of practical interest, it contains much more nonzero elements and can be easily too large to solve. We can reduce the numerical burden by making the coefficient matrix sparser. Bouchon *et al.* (1995) suggested an approach of threshold criterion to remove very small entries in the coefficient matrix for the BE numerical simulation. Encouraging results with significant savings on both computing time and memory requirements were demonstrated by Ortiz-Aleman *et al.* (1998) using various threshold criteria. The approach is based on the significant spatial decay of Green's functions. The interaction between two spatial points separated at large relative distance may be too weak and can be neglected. The thresholding strategy can be directly used in our modeling program. The resultant sparse system is more suited to be solved by conjugate gradient algorithms. Fast convergence rates can be obtained by (1) using the main diagonal part of the coefficient matrix as a preconditioner, and (2) taking the solution at present frequency step as an initial guess for solving the next frequency step. The approximate solution with the thresholding approach is more or less similar to aperture approximation in the Kirchhoff modeling. Some minor reflections and small-amplitude changes imposed on seismic responses are missing, but the main features of seismograms are preserved.

NUMERICAL EXAMPLES

It has been recognized in exploration geophysics that the complex near-surface media can form strong multiple scattered noise that may be extremely deteriorative to seismic data. Likewise in seismic ground motion, the scattering effect of volume heterogeneities of the near-surface media below a rough topography should be considered in the amplification/deamplification evaluation. In this section, we present examples to demonstrate the combined effects of both rough topography and volume heterogeneities in the near-surface layered media. All computations for these examples are performed with frequency range $0 \sim 40$ Hz and the source at depth 20 m below the free surface. The dimensions of the models are 3000 m horizontally and 1000 m vertically. These examples also illustrate the usefulness of our method for investigating the complexity of multiply scattered wavefields in random media.

Fig. 5(a) shows a homogeneous layered model with two upper-rises on the free surface and the wave velocity indicated in the figure. The model is designed to illustrate the scattering effect of rough topography in a homogeneous layered system. From the snapshot shown in Fig. 5(b) calculated at 600 ms, we see strong scattering energy from topographic anomalies. However, the absence of volume heterogeneities leads to a very weak fluctuation in the coherent wavefield within the interior of the model. This is the distinct characteristic compared to wave propagation in the presence of volume heterogeneities.

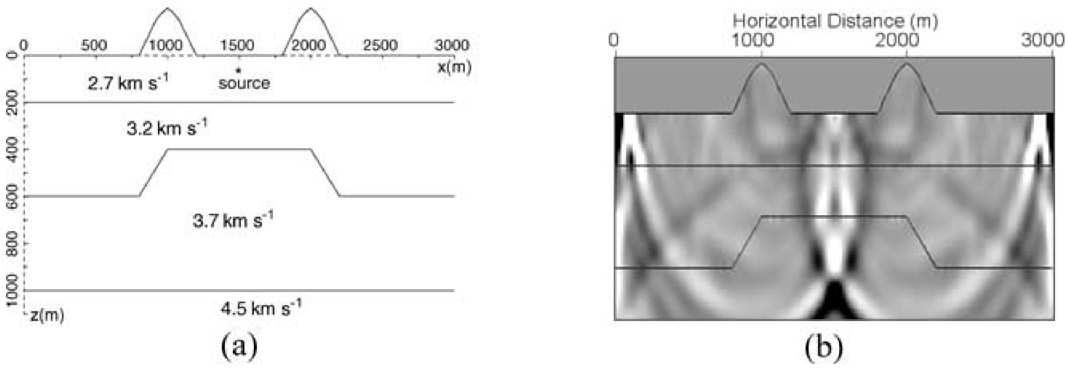

Figure 5. Synthetic seismograms for piecewise homogeneous media. (a) Homogeneous multilayered model with the free surface of two upper-rises. (b) Snapshot of wavefields passing the whole model at 600 ms.

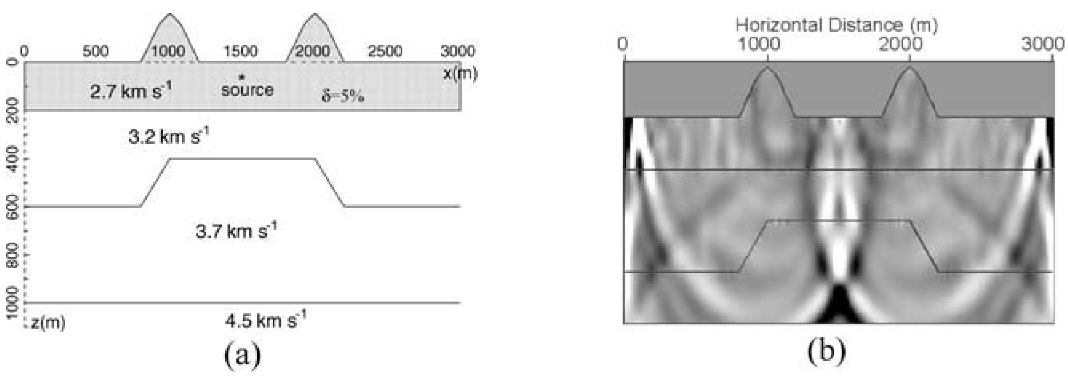

Figure 6. Synthetic seismograms for piecewise heterogeneous media. (a) Heterogeneous multilayered model with randomly 5 per cent velocity perturbation in the near-surface layer. (b) Snapshot of wavefields passing the whole model at 600 ms.

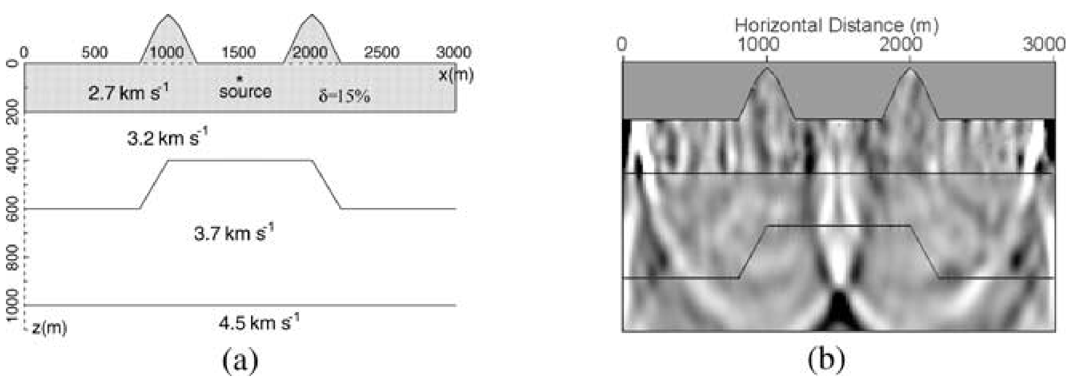

Figure 7. Synthetic seismograms for piecewise heterogeneous media. (a) Heterogeneous multilayered model with randomly 15 per cent velocity perturbation in the near-surface layer. (b) Snapshot of wavefields passing the whole model at 600 ms.

The near-surface sediment is generally a highly heterogeneous region. Let us perturb the medium velocity of the near-surface layer in the model randomly by 5 per cent, as shown in Fig. 6(a), but leave the others in the model intact. We see fairly complex seismic responses (see Fig. 6b) generated due to the diffusion scattering of the volume heterogeneities. The wavefield's interaction with the small-scale heterogeneities poses quite different scattering characteristics from topographic scatterings. The snapshot demonstrates the development of the volume scattering into the interior of the model. The wavefield fluctuation, however, is moderate because of the small velocity perturbation in this example.

The situation becomes formidable when the velocity perturbation increases to 15 per cent (see Fig. 7a). The snapshot shown in Fig. 7(b) exhibits strong scattered noises due to random volume heterogeneities especially in the near-surface layer. These strong diffuse scatterings break up wavefronts, destroy wavefields, and impair the quality of seismic data. Multiple scattering still continues after the primary wave front has passed as time progresses. Although heterogeneities in the near-surface medium are not purely random and may span many different scales, the examples given in this section may provide insight into volume scattering effects by small-scale heterogeneities in the near-surface layer.

CONCLUSION

We have presented a boundary-volume integral equation technique to simulate wave propagation in multilayered media having irregular interfaces and volume heterogeneities in each layer. We first describe wave propagation within each layer by a generalized Lipmann-Schwinger integral equation in terms of volume scattering and boundary scattering. We then extend the integral equation to multilayered media using the boundary conditions of continuity for displacement and traction across all interfaces. The resultant global coefficient matrix is sparse and narrow-banded, depending on the complexity of the model. We discuss several aspects of seismic modeling implementation. Compared to the finite-difference and finite element methods, this method enjoys a distinct characteristic of the explicit use of boundary conditions across subsurface interfaces, and consequently is most suitable to accurately model wave propagation in piecewise heterogeneous media that the Earth presents. Wave propagation in such a medium will dominate the reflections/transmissions at interfaces. To show the applicability of the method, we calculated synthetic seismograms that show significant impact of volume heterogeneities on the seismic response in layered medium system.

ACKNOWLEDGMENTS

This material is based on the research carried out by LYF when he worked first at Dept. of Engineering Mechanics, Tsinghua University, and later at Institute of Tectonics, University of California at Santa Cruz.

REFERENCES

Bouchon, M., Campillo, M. & Gaffet, S., 1989. A boundary integral equation-discrete wavenumber representation method to study wave propagation in multilayered media having irregular interfaces, *Geophysics,* **54**, 1134–1140.

Bouchon, M., Schultz, C.A. & Toksöz, M.N., 1995. A fast implementation of boundary integral equation methods to calculate the propagation of seismic waves in laterally varying layered media, *Bull. seism. Soc. Am.,* **85**, 1679–1687.

Campillo, M., 1987. Modeling of *SH*-wave propagation in an irregularly layered medium—Application to seismic profiles near a dome, *Geophys. Prospect.,* **35**, 236–249.

Chen, X.F., 1990. Seismogram synthesis for multilayered media with irregular interfaces by global generalized reflection/transmission matrices method—I. Theory of two-dimensional *SH* case, *Bull. seism. Soc. Am.,* **80**, 1696–1724.

Coifman, R., Rokhlin, V. & Wandzura, S., 1993. The fast multipole method for the wave equation: a pedestrian prescription, *IEEE Antennas Propagation Mag.,* **35**, 7–12.

Fu, L.Y., 1996. 3-D boundary element seismic modeling in complex geology, *66th Ann. Internat. Mtg., Soc. Expl. Geophys.,* Expanded Abstracts, 1239–1242.

Fu, L.Y., 2000. Numerical study of generalized Lipmann-Schwinger integral equation including surface topography, accepted by *Geophysics.*

Fu, L.Y. & Wu, R.S., 2000. Infinite boundary element absorbing boundary for wave propagation simulations, *Geophysics,* **65**, 625–637.

Fu, L.Y. & Wu, R.S., 2001. A hybrid BE-GS method for modeling regional wave propagation, *Pure appl. Geophys.,* **158**, 1251–1277.

Fu, L.Y., Mu, Y.G. & Yang, H.J., 1997. Forward problem of nonlinear Fredholm integral equation in reference medium via velocity-weighted wavefield function, *Geophysics,* **62**, 650–656.

Fu, L.Y., Wu, R.S. & Campillo, M., 2002. Energy partition and attenuation of regional phases by random free surface, to appear in, *Bull. seism. Soc. Am.*

Fujiwara, H., 2000. The fast multipole method for solving integral equations of three-dimensional topography and basin problems, *Geophys. J. Int.,* **140**, 198–210.

Kennett, B.L.N., 1983. *Seismic Wave Propagation in Stratified Media,* Cambridge University Press, Cambridge.

Kennett, B.L.N., 1984. Guided wave propagation in laterally varying media—I. Theoretical development, *Geophys. J. R. astr. Soc.,* **79**, 235–255.

Ortiz-Alemán, C., Sánchez-Sesma, F.J., Rodriguez-Zuniga, J.L. & Luzon, F., 1998. Computing topographical 3D site effects using a fast IBEM/conjugate gradient approach, *Bull. seism. Soc. Am.,* **88**, 393–399.

Schuster, G.T., 1985. A hybrid BIE + Born series modeling scheme: Generalized Born series, *J. acoust. Soc. Am.,* **77**, 865–879.

Trifunac, M.D., 1971. Surface motion of a semi-cylindrical alluvial valley for incident plane *SH* waves, *Bull. seism. Soc. Am.,* **61**, 1755–1770.

Wu, R.S., 1989. The perturbation method in elastic wave scattering, *Pageoph,* **131**, 605–637.

Wu, R.S. & Fu, L.Y., 1998. A hybrid method for wave propagation simulation in near-surface regions, *68th Ann. Internat. Mtg., Soc. Expl. Geophys.,* Expanded Abstracts, 1065–1068.